Long-chain polyunsaturated fatty acids in the *sn*-2 position of phosphatidylcholine decrease the stability of recombinant high density lipoprotein apolipoprotein A-I and the activation energy of the lecithin:cholesterol acyltransferase reaction

John S. Parks[1] and Abraham K. Gebre

Department of Comparative Medicine, The Bowman Gray School of Medicine of Wake Forest University, Medical Center Boulevard, Winston-Salem, NC 27157-6279

Abstract The lecithin:cholesterol acyltransferase (LCAT) kinetics and activation energy and the stability of apolipoprotein A-I (apoA-I) were investigated using recombinant HDL (rHDL) containing phosphatidylcholine (PC), [^{3}H]cholesterol, and apo A-I. The PC component of the rHDL contained *sn*-1 16:0 and *sn*-2 18:1 (POPC), 20:4 (PAPC), 20:5 n-3 (PEPC), or 22:6 n-3 (PDPC) or 10% of the respective PC species and 90% *sn*-1 18:1, *sn*-2 16:0 PC ether (OPPC ether). The app V_{max} of the rHDL containing 100% PC varied 10-fold and was ordered POPC>PEPC>PAPC>PDPC, whereas the app K_m values varied 19–43 μM PC. The ether-containing rHDL had app V_{max} values 17–40% of their respective 100% PC rHDL, but maintained the same rank order. The activation energy of LCAT was lower for rHDL containing long chain polyunsaturated fatty acids (PUFA) compared to rHDL containing 100% POPC or 10% PC/90% OPPC ether. The concentration of guanidine HCl ($D_{1/2}$) required to denature one-half of the apoA-I on rHDL containing long chain PUFA was reduced (1.2–1.6 M) compared to those containing 100% POPC or 10% PC/90% OPPC (2.2–2.4 M) and there was a strong correlation (r^2 = 0.71) between LCAT activation energy and the stability of apoA-I (i.e., $D_{1/2}$). We conclude that long chain PUFA in the *sn*-2 position of PC decreases the catalytic efficiency of LCAT, the activation energy of the LCAT reaction and the stability of apoA-I on the rHDL particles. The strong association between rHDL apoA-I stability and LCAT activation energy suggests that the temperature-dependent step of the LCAT reaction may be sensitive to the strength of the interaction of apoA-I with rHDL PC.—**Parks, J. S., and A. K. Gebre.** Long-chain polyunsaturated fatty acids in the *sn*-2 position of phosphatidylcholine decrease the stability of recombinant high density lipoprotein apolipoprotein A-I and the activation energy of the lecithin:cholesterol acyltransferase reaction. *J. Lipid Res.* 1997. **38:** 266–275.

Supplementary key words cholesterol • POPC • PAPC • PEPC • PDPC • OPPC ether

Lecithin:cholesterol acyltransferase (LCAT) is a 63–65 kD plasma glycoprotein that is responsible for the synthesis of most cholesterol esters (CE) found in plasma (1). The enzyme catalyzes the hydrolysis of a *sn*-2 fatty acid from phospholipid and the transesterification of the fatty acid to the 3-hydroxyl group of cholesterol to form CE and lysophospholipid (1). Apolipoprotein A-I (apoA-I) serves as a cofactor for the reaction and is the major structural apolipoprotein of high density lipoproteins (HDL), which are the preferred macromolecular substrate particle for the LCAT reaction (2–4). LCAT is essential for the maturation of HDL that are secreted from the liver and intestine or formed during lipolysis of triglyceride-rich lipoproteins (5). The generation of CE by LCAT converts nascent discoidal HDL to spherical particles, which are the predominant form of HDL in plasma. The importance of LCAT in this HDL maturation process is best illustrated by genetic (6) or induced (7) LCAT deficiency states in

Abbreviations: PUFA, polyunsaturated fatty acids; PC, phosphatidylcholine; CE, cholesteryl ester; LCAT, lecithin:cholesterol acyltransferase; apoA-I, apolipoprotein A-I; rHDL, recombinant HDL; ($D_{1/2}$), concentration of guanidine HCl required to denature one half of the apoA-I on rHDL; HDL, high density lipoprotein; LDL, low density lipoprotein; LysoPC, 1-palmitoyl-*sn*-glycero-3-phosphocholine; OPPC ether, 1-oleyl-2-palmityl phosphatidylcholine ether; POPC, 1-palmitoyl-2-oleoyl-*sn*-glycero-3-phosphocholine; PAPC, 1-palmitoyl-2-arachadonoyl-*sn*-glycero-3-phosphocholine; PEPC 1-palmitoyl-2-eicosapentaenoyl-*sn*-glycero-3-phosphocholine; PDPC, 1-palmitoyl-2-docosahexaenoyl-*sn*-glycero-3-phosphocholine; (ΔG^0d), free energy of denaturation at zero guanidine HCl concentration; Ea, activation energy.

[1]To whom correspondence should be addressed.

which nascent discoidal HDL accumulate in plasma and CE concentrations are very low. LCAT is also thought to play an important role in reverse cholesterol transport, the process by which excess free cholesterol is removed from peripheral tissues by HDL and transported to the liver for excretion (1). The role of LCAT in this process appears to be the generation of a chemical gradient for the flux of free cholesterol from cells into HDL by decreasing the concentration of free cholesterol in HDL through its conversion to CE.

Studies of the enzymatic mechanism of LCAT have been significantly advanced by the ability to form discoidal substrates of known composition that mimic nascent HDL in size and composition (8). These are referred to as recombinant HDL (rHDL) and are made by a cholate dialysis procedure (9). Using rHDL, investigators showed that LCAT activity in vitro can vary 100-fold depending on the fatty acyl composition of rHDL (10). This variation in LCAT activity could be mediated through changes in enzyme binding to the interface of the rHDL particle and/or through changes in the binding and catalysis of monomeric substrate lipids (i.e., cholesterol and phospholipid). Studies by Jonas et al. (10) and Pownall, Pao, and Massey (11) used ether phosphatidylcholine (PC) analogues, which cannot be hydrolyzed by LCAT, to form rHDL that contained a uniform, inert interface to distinguish between interfacial versus active site effects of various PC species on LCAT activity. These studies demonstrated that systematically changing the fatty acyl composition of PC modulated LCAT activity through changes in the interfacial binding of LCAT to rHDL as well as changes in the binding and catalysis of substrate molecules at the active site of the enzyme. These studies have increased our mechanistic understanding of the control of LCAT enzymatic activity.

The purpose of this study is to better understand the mechanism by which long-chain polyunsaturated fatty acids affect LCAT activity. The impetus for the present study originated with the observation that feeding nonhuman primates a diet in which fish oil was isocalorically substituted for lard resulted in a decreased concentration of CE in plasma LDL and HDL (12). Plasma LCAT mass and activity, measured with rHDL-containing egg yolk PC, were the same for both diet groups (13). However, when phospholipids from the plasma of both diet groups were extracted, purified, and used to make rHDL, the LCAT activity of rHDL made from phospholipids derived from the plasma of the fish oil group was less than half that of the lard group (13). Later studies using defined, synthetic PC species demonstrated that n-3 fatty acids in the *sn*-2 position of PC were responsible for the decreased reactivity of plasma LCAT (14). However, mechanistic details for the decreased reactivity of LCAT with n-3 fatty acids are lacking and are the subject of this study.

EXPERIMENTAL PROCEDURES

Materials

The following reagents were purchased from Sigma Chemical Co. (St. Louis, MO); *cis*-5,8,11,14,17-eicosapentaenoic acid (EPA), *cis*-4,7,10,13,16,19-docosahexaenoic acid (DHA), 1-palmitoyl-*sn*-glycero-3-phosphocholine (LysoPC), 4-dimethylaminopyridine, *cis*-5,8,11,14-eicosatetraenoic acid, 1-palmitoyl-2-oleoyl-*sn*-glycero-3-phosphocholine (POPC), sodium cholate, and ultrapure guanidine-HCl. N,N′-dicyclohexylcarbodiimide and 2,6-di-tert-butyl-4-methylphenol (butylated hydroxytoluene, BHT) were purchased from Aldrich Fine Chemicals (Milwaukee, WI). Radiolabeled cholesterol ([7-^{3}H]cholesterol; 21.8 Ci/mmol) was obtained from DuPont/New England Nuclear (Boston, MA). OPPC ether (1-oleyl-2-palmityl phosphatidylcholine ether) was purchased from Serdary Research Labs (London, Ontario, Canada). Cholesterol was obtained from Nu Chek Prep, Inc. (Elysian, MN). All other reagents, chemicals, and solvents were purchased from Fisher Scientific Co. (Pittsburgh, PA).

PC synthesis and rHDL formation

PC species were synthesized from 1-palmitoyl lyso PC and the appropriate fatty acid as described previously (14, 15). PC species were characterized by thin-layer chromatography (14) and repurified by HPLC prior to rHDL formation when a homogeneous band was not observed on thin-layer chromatography. The HPLC procedure for PC purification used a silica gel column (25 × 0.46 cm Partisil 5 silica; Phenomenex, Torrance, CA) and a gradient elution consisting of mixtures of solvent A (98.5% isopropanol–hexane 8:6 and 1.5% water) and solvent B (91% isopropanol–hexane 8:6 and 9% water). The following gradient was used: 85% A/15% B for 10 min, 27% A/73% B for 8 min, 100% B for 24 min, and 85% A/15% B for 13 min. Elution was monitored as absorbance at 208 nm and fractions were collected, pooled, dried under N_2, and redissolved in $CHCl_3$. PC species were protected from oxidation by addition of BHT (0.02 wt% final concentration relative to PC) and by storage under argon atmosphere.

rHDL were made by the cholate dialysis procedure originally described by Matz and Jonas (8) as modified by Parks, Thuren, and Schmitt (14). For the present study rHDL were used with a starting molar composition of PC:[^{3}H]cholesterol (50,000 dpm/μg):apoA-I =

80:5:1. In some experiments a starting composition of 55:3:1 was used. In some cases the rHDL at the same PC:cholesterol:apoA-I molar ratio contained 90% OPPC ether and 10% of the various PC species were studied rather than 100% of the test PC. These rHDL were used to examine LCAT reaction kinetics using particles with a uniform interfacial surface. The size distribution of rHDL was determined using 4–30% polyacrylamide gradient gels run for 1700 V-h (16). The gels were scanned using a Zeineh laser densitometer (Biomed Instruments, Fullerton, CA) and the data were processed according to the method of Verdery et al. (17). rHDL that contained a small amount of lipid free apoA-I were repurified on a Superose 12B HPLC column (1.6 × 50 cm) equilibrated with 10 mM Tris, 140 mM NaCl, 0.01% EDTA, 0.01% NaN_3, pH 7.4 (flow rate = 1 ml/min).

Purification of plasma LCAT

LCAT was purified from fresh recovered human plasma obtained from the Red Cross as described previously (18). This procedure resulted in pure LCAT as determined by SDS-PAGE (18) at a concentration of 50 μg/ml (19, 20). The specific activity of the purified LCAT using rHDL containing POPC:cholesterol:apoA-I (70:5:1 molar ratio) was approximately 54 nmol CE formed/h per μg using the assay conditions given below.

LCAT incubations

LCAT incubations were performed in duplicate in 0.5 ml buffer (10 mM Tris, 140 mM NaCl, 0.01% EDTA, 0.01% NaN_3, pH 7.4) containing: rHDL (1.0–225 μg PC), 0.6% bovine serum albumin (fatty acid-free), 2 mM β-mercaptoethanol, and 25 ng pure LCAT as described previously (18). Control incubations contained all constituents except LCAT. Tubes were gassed with argon and incubated at 37°C for various times between 10 min and 2 h. Control experiments showed that CE formation was linear up to 2 h using our experimental conditions provided CE formation was <25%. The average error between duplicate assays was 8.5% (n = 28). Apparent V_{max} and K_m values for cholesterol esterification were determined from a nonlinear least squares fit of the substrate saturation data to the Michaelis-Menten equation [activity = $(V_{max} \times \mu M\ PC)/(K_m + \mu M\ PC)$] using a BMDP statistical program (Los Angeles, CA).

Activation energy for CE formation by LCAT was determined from Arrhenius plots of LCAT reactions performed at different temperatures. Reactions were performed using 25 μg rHDL substrate PL and 25 ng pure LCAT as described above. The incubation time ranged from 10 min to 2 h depending on the type of PL in the rHDL. The reactions were performed at 37, 34, 31, 28, and 25°C as described above. Arrhenius plots were constructed as the reciprocal of incubation temperature in degrees Kelvin versus log CE formation in nmol/h per ml LCAT. The line of best fit was determined using linear regression analysis and the slope of the line was used to calculate activation energy according to the formula: Ea (cal/mol) = −2.3R (slope), where R equals the gas constant (1.987 $cal/deg^{-1}/mole^{-1}$).

Circular dichroism measurements

The stability of rHDL apoA-I in the presence of increasing concentrations of guanidine HCl was measured by monitoring ellipticity at 222 nm, which is indicative of α-helical content of rHDL apoA-I. Ten μg of rHDL protein was incubated with 0–6 M guanidine HCl in buffer (200 μl final volume) for at least 48 h at room temperature under an argon atmosphere. The guanidine HCl concentration was varied using an 8 M stock solution of ultra-pure guanidine HCl. The samples and blanks were then loaded into a 0.1-cm quartz cell and scanned 5 times from 223 to 221 nm in a Jasco 720 spectropolarimeter (Jasco, Inc., Easton, MD) using the following conditions: band width = 1 nm; response time = 2 s; and scan speed = 20 nm/min. Five scans of each sample were averaged and the average ellipticity at 222 nm was read using a screen cursor on the computer. The appropriate blank for each guanidine HCl concentration was subtracted from the samples and the ellipticity values (mdeg) were converted to mean residue ellipticity ($deg \cdot cm^2 \cdot decimole^{-1}$) according to the following formula: $[\theta] = \theta/10\ CL$, where $[\theta]$ = mean residue ellipticity; θ = ellipticity (mdeg); C = residue molar concentration (i.e., molar concentration of apoA-I × 243 amino acid residues/mole); and L = path length of the cell in cm. The percentage α-helical content of rHDL apoA-I was calculated by the equation of Chen, Yang, and Martinez (21).

A plot of mean residue ellipticity versus guanidine HCl concentration for each rHDL was constructed. The concentration of guanidine HCl at which denaturation of apoA-I was half completed ($D_{1/2}$) was determined graphically from each plot. The standard free energy of denaturation (ΔG^0_d) was derived according to the method of Sparks, Lund-Katz, and Phillips (22) based on the denaturant binding model described by Pace (23).

RESULTS

Chemical composition and particle size characterization of the rHDL used for the present study are shown

TABLE 1. Chemical composition of rHDL

rHDL PC	PC:Chol:ApoA-I	Stokes' Radius of Major Peak
	molar ratio	*nm*
100% POPC	70:4.7:1	4.6
100% PAPC	61:3.0:1	4.6-4.8
100% PEPC	59:3.5:1	4.5
100% PDPC	60:2.8:1	4.5
10% POPC/90% OPPC ether	70:4.6:1	5.0
10% PAPC/90% OPPC ether	75:4.7:1	4.9
10% PEPC/90% OPPC ether	74:4.5:1	4.9
10% PDPC/90% OPPC ether	71:4.7:1	4.9

Data are from a representative set of rHDL. Procedures for determination of chemical composition have been published (14). Stokes' radius was determined by electrophoresis using 4–30% polyacrylamide gradient gels. rHDL containing 10% PC/90% OPPC ether were reisolated by HPLC on a Superose 12B column as described in the Methods section.

in **Table 1.** The chemical compositions were less variable among rHDL containing a uniform interfacial surface of 90% OPPC ether compared to those containing 100% PC. Overall, the chemical compositions among all of the particles were similar (PC: cholesterol: apoA-I molar ratio [mean ± SD] = 68 ± 6: 4.1 ± 0.8: 1). Gradient gel electrophoresis profiles showed a major population of rHDL with a Stokes' radius of 4.6–5.0 nm for all preparations. In general, minor subpopulations were more prevalent in the 100% PC rHDL (i.e., 5.8, 4.2, and 3.9 nm) compared to the rHDL containing 90% OPPC ether. The rHDL containing n–3 fatty acids in the *sn*-2 position (i.e., 100% PEPC and PDPC) were slightly smaller (4.5 vs. 4.6 nm) than those containing POPC or PAPC (Table 1). In addition, the OPPC ether-containing rHDL were slightly larger than those containing 100% PC.

Substrate saturation curves for CE formation by LCAT were performed with the various rHDL (**Fig. 1**). Based on pilot experiments the incubation time for each rHDL was adjusted to keep the CE formation in a linear range (<25% CE formation). The 100% PC rHDL showed an order of reactivity that was: POPC>PEPC>PAPC>PDPC. The reaction rates for the OPPC ether-containing rHDL were 20–40% those of the pure PC rHDL, as would be expected as 90% of the interfacial surface of the rHDL was inert to LCAT. The order of reactivity of the OPPC ether rHDL was the same as the 100% PC rHDL.

The kinetic data were analyzed by nonlinear least squares analysis to determine the apparent maximal velocity (appV_{max}) and apparent K_m (appK_m) of the cholesterol esterification reaction. The results are presented in **Table 2.** With respect to the 100% PC rHDL, the appV_{max} values varied 10-fold and for PAPC, PEPC, and PDPC were 34%, 61%, and 10% that of POPC, respectively. However, the appK_m values for rHDL containing 100% PC were similar to each other and ranged from 19 to 43 μM PC. The overall result was a catalytic efficiency of LCAT (appV_{max}/K_m) for PC species containing long chain polyunsaturated fatty acids that was 7–26% that of POPC.

The kinetic results for the OPPC ether-containing rHDL are also shown in Table 2. The V_{max} for the ether-containing complexes was 23–62% that of the respective 100% PC complexes, but the same rank order of the V_{max} values was apparent for both the 100% PC and 90% OPPC ether rHDL. In general, the appK_m values

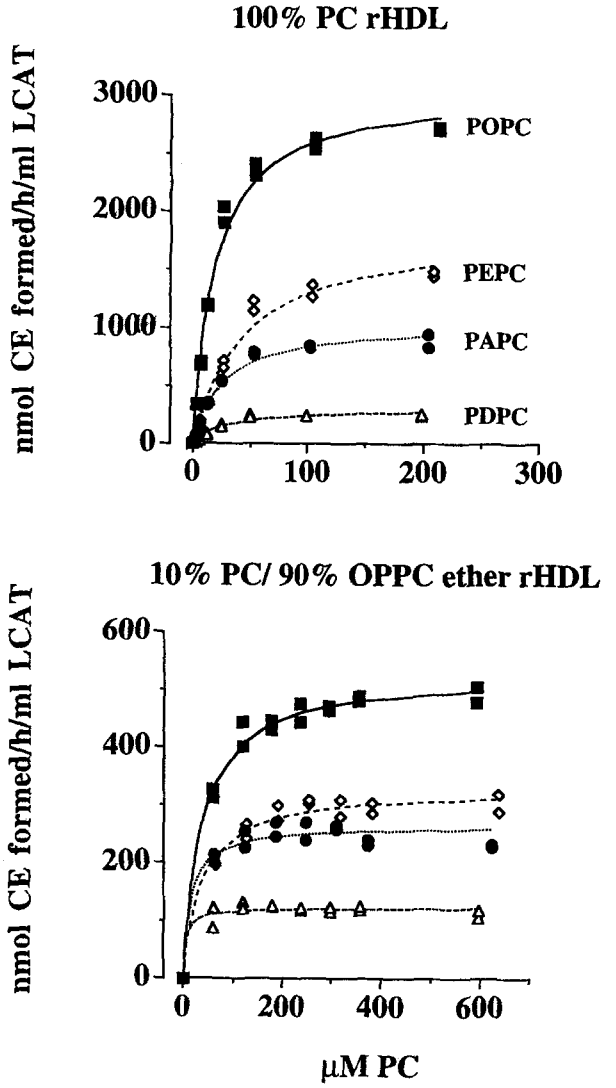

Fig. 1. Substrate saturation curves for CE formation by LCAT. LCAT incubations were performed as described in the Methods section. Duplicate values are shown for each substrate concentration (in some cases the symbols overlap). The line of best fit, determined by a nonlinear least squares analysis fit of the data to the Michaelis-Menten equation, is also shown for each rHDL.

TABLE 2. Effect of *sn*-2 fatty acyl group of PC on rHDL LCAT kinetic constants and activation energy

PC Type	App V_{max} (nmol CE/h/ml LCAT)	App K_m (μM PC)	App V_{max}/App K_m (nmol CE/h/ml LCAT/μM PC)	Activation Energy (kcal/mol)
100% POPC	3054 ± 84	19 ± 2	164	16.3
100% PAPC	1046 ± 44	25 ± 3	42	14.9
100% PEPC	1849 ± 117	43 ± 7	43	8.4
100% PDPC	306 ± 21	27 ± 6	11	12.9
10% POPC/90% ether	528 ± 9	36 ± 4	15	19.9
10% PAPC/90% ether	264 ± 9	15 ± 6	18	20.9
10% PEPC/90% ether	329 ± 9	36 ± 6	9	18.9
10% PDPC/90% ether	122 ± 5	6 ± 6	20	22.1

Kinetic constants (app V_{max} and app K_m) were determined from a nonlinear least squares analysis of the substrate saturation curves in Fig. 1. Standard deviations of the parameter estimates based on the curve fitting are shown. The activation energy was derived from the slope of the Arrhenius plots as described in the Methods section. The average error in estimation of the slope by linear regression analysis was 9% (n = 8).

for the rHDL were similar to each other and agreed closely with those of the 100% POPC rHDL. Only the 10% PDPC rHDL had an apparently lower value compared to the other rHDL. The app V_{max}/ K_m values were similar among complexes and range from 9 to 20 nmol/hr per ml · μM for the 10% PC/90% OPPC ether rHDL.

The activation energy for the cholesterol esterification reaction of LCAT was determined from the slope of the Arrhenius plots and the values are reported in Table 2. The activation energy was lower for the 100% PC rHDL containing long-chain polyunsaturated fatty acids, particularly PEPC. However, the activation energies were more uniform for the rHDL containing OPPC ether. There was also relatively close agreement between the activation energies of the POPC and the OPPC ether-containing rHDL.

As apoA-I is an activator of the LCAT reaction and the activation energy varied among the 100% PC rHDL, we investigated the interaction of apoA-I with PC among the various rHDL. It is well known that the α-helical content of apoA-I increases upon binding to phospholipid. Therefore, we investigated the strength of the interaction between apoA-I and PC by adding increasing concentrations of the denaturant guanidine HCl and monitoring the decrease in ellipticity at 222 nm, a sensitive measurement of the α-helical content of proteins using circular dichroism spectroscopy. The results are shown in **Fig. 2.** Note that the denaturation curves for the 100% PC rHDL containing long chain polyunsaturated fatty acids were shifted to the left compared to POPC rHDL, indicating that less guanidine HCl was required to denature the apoA-I on these particles. However, as shown in the bottom panel of Fig. 2, the denaturation curves for the OPPC ether-containing rHDL were similar to one another and were similar to the curve for 100% POPC rHDL (upper panel). These data suggested that the type of fatty acid in the *sn*-2 position of PC affected the stability of the interaction between apoA-I and PC.

Using the denaturant binding model of Pace (23), we determined the free energy of denaturation at zero guanidine HCl concentration (ΔG^0_d) for rHDL apoA-I. The results are shown in **Table 3** along with the midpoint of the guanidine HCl denaturation curve, the calculated moles of guanidine HCl bound per mole apoA-I, and the calculated α-helical content of the rHDL apoA-I. ΔG^0d for the rHDL containing 100% PC with long chain polyunsaturated fatty acids was 27–50% that of rHDL containing 100% POPC. However, there was close agreement in the ΔG^0d for rHDL containing 100% POPC and those containing 10% PC/90% OPPC ether. The concentration of the guanidine HCl necessary to achieve one-half denaturation of the rHDL apoA-I also was less for the particles containing long-chain polyunsaturated PC species (1.2–1.6 M) compared to POPC (2.2 M) or to rHDL containing 10% PC/90% OPPC ether (2.2–2.4 M). The amount of guanidine HCl bound to apoA-I was similar among the rHDL except for the rHDL containing 100% PDPC, which was lower than the others. Similar results were obtained for the denaturation of rHDL with a starting molar ratio of PC:cholesterol:apoA-I of 50:2.5:1 (data not shown). The percentage of α-helical content of apoA-I was similar among all rHDL (62–67%) except that for 100% POPC, which was slightly higher compared to the others (71%).

To investigate the relationship between rHDL apoA-I stability and activation of the LCAT reaction by apoA-I, we made a plot of activation energy versus $D_{1/2}$ and ΔG^0_d (**Fig. 3**). There was a strong positive relationship between the activation energy of the LCAT reaction and the concentration of guanidine HCl needed for one-half denaturation of rHDL apoA-I (r^2 = 0.71).

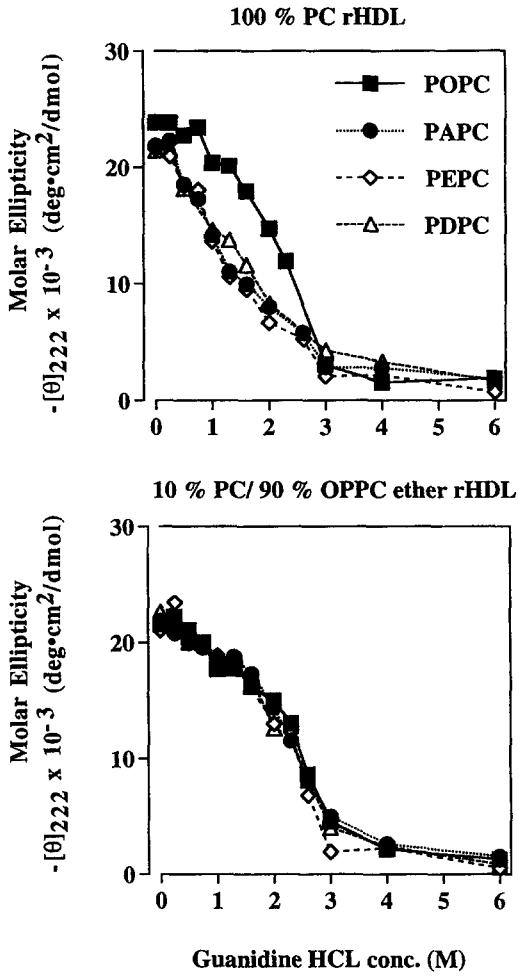

Fig. 2. Guanidine HCl denaturation curves of rHDL monitored by circular dichroism spectroscopy. rHDL (10 μg protein) were adjusted to various final concentrations of guanidine HCl and incubated for at least 48 h at room temperature under an argon atmosphere before determining the ellipticity at 222 nm. Details of the procedure are given in the Methods section.

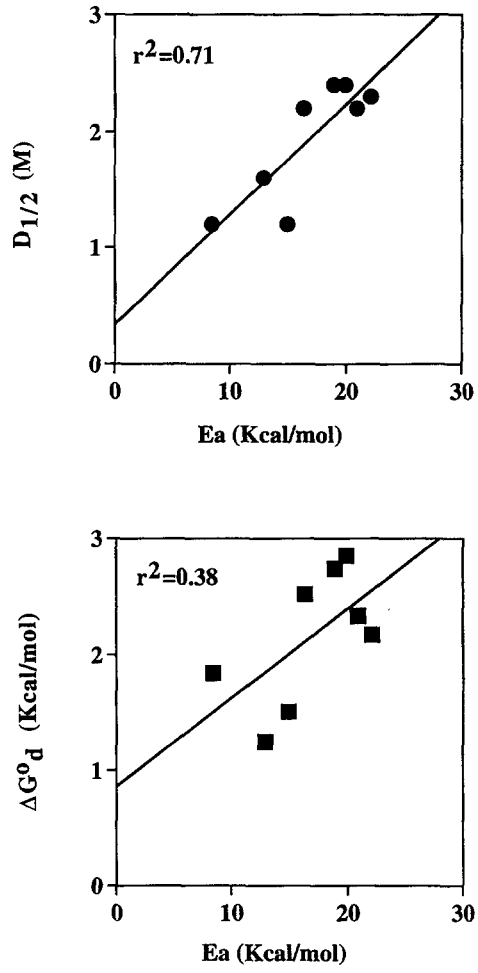

Fig. 3. Plots of activation energy (Ea) for CE formation by LCAT versus the concentration of guanidine HCl necessary to denature one-half of the apoA-I on rHDL ($D_{1/2}$; top panel) and the free energy of denaturation at zero guanidine HCl concentrations (ΔG^0d; bottom panel). Each point represents data from an individual rHDL complex; the line of best fit, determined by linear regression analysis, is shown for each plot.

TABLE 3. Effect of *sn*-2 fatty acyl group of PC on rHDL apoA-I stability

rHDL PC	ΔG^0_d	$D_{1/2}$ (M)	mol Guanidine HCl per mol ApoA-I	% α-Helix
	kcal/mol			
100% POPC	2.52	2.2	8.4	71
100% PAPC	1.51	1.2	7.1	65
100% PEPC	1.84	1.2	7.8	64
100% PDPC	1.25	1.6	5.5	63
10% POPC/90% OPPC ether	2.85	2.4	9.4	63
10% PAPC/90% OPPC ether	2.33	2.2	7.9	64
10% PEPC/90% OPPC ether	2.74	2.4	9.1	62
10% PDPC/90% OPPC ether	2.17	2.3	7.5	67
ApoA-I	2.2	1.1	10.3	47

Values are derived from the guanidine HCl denaturation study in Fig. 2 using the denaturant binding model described previously (22, 23). The percentage of α-helical content was calculated from the mean residue ellipticity at 222 nm using the formula of Chen et al. (21). The coefficient of variation for the circular dichroism results was 13% for separate experiments (n = 4) performed on different days.

There also was a significant, though somewhat weaker correlation, between activation energy and the free energy of denaturation at zero guanidine HCl (r^2 = 0.376).

DISCUSSION

Previous studies have shown that PC species containing long chain PUFA in the *sn*-2 position react poorly with LCAT (13, 14, 24). The purpose of this study was to investigate the mechanism of this poor reactivity. Using rHDL of comparable size and composition containing defined PC species or containing an interface of 90% OPPC ether and 10% of the defined PC species, we investigated the reaction kinetics of CE formation by LCAT and the activation energy and the stability of apoA-I on rHDL. Our data show that the low reactivity of LCAT to long-chain PUFA is due to several factors, including a decrease in appV_{max} for CE formation by LCAT and a decreased stability or association of apoA-I for the rHDL surface, with only minor differences in appK_m. We also found a strong association between LCAT activation energy and the stability of apoA-I for the rHDL surface. Taken together, these observations suggest that the poor LCAT reactivity for long-chain PUFA is multifactorial, involving turnover of substrate molecules at the active site of the enzyme and activation of the enzyme by its cofactor apoA-I.

The kinetic analysis of the LCAT reaction using 100% PC and 10% PC/90% OPPC ether rHDL suggested a similar mechanism for the poor reactivity of n-3 versus n-6 fatty acids. For this study we focused on PEPC and PDPC, as representative PC species containing n-3 fatty acids, and on PAPC, as a representative PC containing n-6 fatty acid, because these PC species are found in plasma HDL when nonhuman primates are fed diets containing n-3 or n-6 fatty acids (13, 24) and 20:5 n-3 and 20:4 n-6 are similar in molecular structure. All three PC species showed decreased catalytic efficiency (i.e., appV_{max}/K_m) relative to POPC-containing rHDL. The decrease in catalytic efficiency was due primarily to a decrease in the appV_{max} with little change in appK_m regardless of whether the PC species contained n-3 or n-6 fatty acids.

As substitution of a uniform, inert rHDL interface with 90% OPPC ether had little effect on the appK_m, it is likely that the rHDL surface containing n-3 or n-6 fatty acids had minor effects on LCAT interfacial binding. Bolin and Jonas (25), using direct binding assays of LCAT to rHDL, have shown that the appK_m of the LCAT reaction reflects interfacial binding affinity, whereas the appV_{max} reflects the active site preference of the enzyme. The appV_{max} difference among PC species was apparent for 100% PC and 10% PC/90% OPPC ether rHDL, whereas the appK_m values were similar among all rHDL investigated except for 10% PDPC/90% OPPC ether rHDL. Taken together, these observations suggest that the decreased reactivity of LCAT for long-chain PUFA does not involve a decrease in interfacial binding of LCAT to the rHDL surface containing n-3 fatty acids, but rather a decreased preference of LCAT for long-chain PUFA at the active site of the enzyme.

We also found that PC containing long-chain PUFA decreased the stability of rHDL apoA-I. rHDL containing PAPC, PEPC, and PDPC had ΔG^0d and $D_{1/2}$ values that were 60% that of POPC with only minor variations in the α-helical content of apoA-I (Table 3). However, there was no difference in these values when the rHDL surface was made uniform with 90% OPPC ether. Several studies have shown that the stability of rHDL apoA-I is dependent on the size of the rHDL particle (22, 26), the cholesterol content (27), the neutral lipid content (28), and whether the rHDL is discoidal or spherical (22, 29). It has also been shown that there is no relationship between the α-helical content of apoA-I and the stability of apoA-I in discoidal rHDL containing cholesterol (27, 28). However, there is little information regarding the influence of PC fatty acyl composition on rHDL apoA-I stability, except for the observation that apoA-I stability is similar for rHDL of comparable size and composition containing POPC versus dimyristoyl PC (22). The most likely explanation for the decreased stability of apoA-I on small HDL is an increase in charge repulsion that results when adjacent α-helical segments of apoA-I come in close contact with each other and decrease their contact with PC (22). The rHDL used in our study were similar in size and chemical composition (Table 1), so that small differences in these variables are unlikely to explain the rather large differences in apoA-I stability observed among rHDL. In addition, we have observed similar results for purified rHDL that exhibit no apparent size heterogeneity (K. Huggins, A. Gebre, and J. Parks, unpublished studies).

The molecular explanation for the decreased interaction of apoA-I with PC species containing long-chain PUFA likely results from the increased polarity and disorder of the PUFA chains. NMR and fluorescence studies have shown that PC species containing PUFA are more hydrated along the fatty acyl chain, are more disordered, and contain a larger free volume (30, 31). Monolayer force-area curves also confirm that PEPC and PDPC have a larger molecular surface area compared to that of POPC (15). This could result in a decreased interaction of apoA-I α-helices with PUFA PC and an increased likelihood of interaction between ad-

jacent antiparallel α-helical segments, which would preserve the α-helical content of apoA-I. Several studies have shown that increasing the PUFA content of membranes alters protein kinase C activity and metarhodopsin formation (32, 33). Additional studies are underway to elucidate the specific molecular interactions between apoA-I and PC species containing long-chain PUFA.

The long-term structural stability of rHDL can be predicted by the free energy of denaturation at zero denaturant concentration (ΔG^0d). Sparks et al. (28) have shown that rHDL with ΔG^0d values less than that of lipid free apoA-I (i.e., 2.4 kcal/mol; (27)) are less stable in long-term storage than those with values greater than apoA-I. We have observed a similar phenomenon in our study. Upon gradient gel analysis of the remainder of our rHDL complexes approximately six months after completion of the reported studies, we observed the breakdown of rHDL containing PEPC, PAPC, and PDPC into larger and smaller particles, whereas the rHDL containing 10% PC/90% OPPC ether and 100% POPC showed minimal changes in size. The three rHDL that lost structural integrity had ΔG^0d values ranging from 1.25 to 1.84 kcal/mol (Table 3), which is less than that of lipid-free apoA-I. While not a systematic investigation, our results do support the findings of Sparks et al. (28) and suggest that rHDL with ΔG^0d values less than that of lipid-free apoA-I are thermodynamically unstable.

A surprising finding of this study was the strong correlation between the activation energy of CE formation of LCAT and the stability of rHDL apoA-I. This relationship was observed using both ΔG^0d and $D_{1/2}$ values. We also noted that the rHDL containing PAPC, PEPC, and PDPC had a lower appV_{max}, as well as lower activation energies relative to that of POPC. This result seemed counterintuitive, as the rHDL with lower activation energies were less reactive with LCAT. We speculate that the temperature-dependent step of the LCAT reaction is the activation of the enzyme by apoA-I, and that this activation is related to the strength of the association between apoA-I and PC. Thus, the stronger the association of apoA-I and PC, the higher the activation energy. The explanation for the decreased appV_{max} in the face of a decreased activation energy likely reflects the active site preference of LCAT for the PC species. Jonas et al. (10) have also reported decreased LCAT reaction rates and activation energy for rHDL containing two PUFA chains, such as *sn*-1, *sn*-2 18:2 PC and *sn*-1, *sn*-2 20:4 PC. These data together suggest that the temperature-dependent step of the LCAT reaction is sensitive to the strength of the PC/apoA-I interaction. Whether this is a direct effect of apoA-I with the "activated" PC substrate or an independent effect of the PC/apoA-I association on the conformation of apoA-I is unknown.

An alternative explanation for the decreased activation energy of the rHDL containing PUFA may be related to the physical chemical properties of the fatty acyl chains. PC species containing PUFA in the *sn*-2 position are less ordered than those containing monounsaturated fatty acids (30, 31, 34). If activation of a PC molecule for the LCAT reaction involves disordering of the PC molecule from the bulk PC, then less energy would be required to activate a PC containing PUFA. Thus, the lower activation energy would be an intrinsic property of the PC molecule based on its fatty acyl composition and not necessarily related to its interaction with apoA-I.

We believe our findings may have physiological implications regarding plasma HDL concentrations and HDL subfraction distribution. We have repeatedly observed that nonhuman primates fed diets enriched in n-3 or n-6 PUFA have lower HDL cholesterol concentrations (12, 24, 35, 36). Similar findings have been observed in human subjects (37, 38). The HDL subfraction distribution also is skewed towards smaller subfractions when PUFA diets are fed (12, 39, 40). This profile may result because apoA-I on HDL precursor particles containing PUFA is less stable and these particles are converted to mature spherical HDL more slowly due to a sluggish LCAT reaction. This scenario may lead to the dissociation of apoA-I from HDL precursor particles because of its reduced thermodynamic stability and incomplete conversion to mature HDL. The dissociated apoA-I may then be hypercatabolized, as has been suggested for lipid-free apoA-I (41, 42), ultimately leading to decreased concentrations of HDL in plasma. Our data in nonhuman primates support this hypothesis, as animals fed a safflower oil diet enriched in 18:2 had a significantly greater fractional catabolic rate for HDL apoA-I compared to those fed a butter diet (43).

The authors gratefully acknowledge the assistance of Linda Odham in manuscript preparation, the editorial comments of Karen Klein, and the statistical advice of Dr. Timothy Morgan, Department of Public Health Sciences. This work was supported by NIH grant HL 49373.

Manuscript received 8 July 1996 and in revised form 7 November 1996.

REFERENCES

1. Glomset, J. A. 1968. The plasma lecithin:cholesterol acyltransferase reaction. *J. Lipid Res.* **9:** 155–167.
2. Fielding, C. J., V. G. Shore, and P. E. Fielding. 1972. A protein cofactor of lecithin:cholesterol acyltransferase. *Biochem. Biophys. Res. Commun.* **46:** 1493–1498.
3. Jonas, A., S. A. Sweeny, and P. N. Herbert. 1984. Discoidal complexes of A and C apolipoproteins with lipids and their reactions with lecithin:cholesterol acyltransferase. *J. Biol. Chem.* **259:** 6369–6375.

4. Jonas, A. 1986. Synthetic substrates of lecithin:cholesterol acyltransferase. *J. Lipid Res.* **27:** 689–698.
5. Atkinson, D., and D. M. Small. 1986. Recombinant lipoproteins: implications for structure and assembly of native lipoproteins. *Annu. Rev. Biophys. Biophys. Chem.* **15:** 403–456.
6. Glomset, J. A., K. R. Norum, and W. King. 1970. Plasma lipoproteins in familial lecithin:cholesterol acyltransferase deficiency: lipid composition and reactivity in vitro. *J. Clin. Invest.* **49:** 1827–1837.
7. Auerbach, B. J., and J. S. Parks. 1989. Lipoprotein abnormalities associated with lipopolysaccharide-induced lecithin:cholesterol acyltransferase and lipase deficiency. *J. Biol. Chem.* **264:** 10264–10270.
8. Matz, C. E., and A. Jonas. 1982. Micellar complexes of human apolipoprotein A-I with phosphatidylcholines and cholesterol prepared from cholate-lipid dispersions. *J. Biol. Chem.* **257:** 4535–4540.
9. Jonas, A. 1986. Reconstitution of high-density lipoproteins. *Methods Enzymol.* **128:** 553–582.
10. Jonas, A., N. L. Zorich, K. E. Kezdy, and W. E. Trick. 1987. Reaction of discoidal complexes of apolipoprotein A-I and various phosphatidylcholines with lecithin:cholesterol acyltransferase. Interfacial effects. *J. Biol. Chem.* **262:** 3969–3974.
11. Pownall, H. J., Q. Pao, and J. B. Massey. 1985. Acyl chain and headgroup specificity of human plasma lecithin:cholesterol acyltransferase. Separation of matrix and molecular specificities. *J. Biol. Chem.* **260:** 2146–2152.
12. Parks, J. S., J. A. Martin, B. L. Sonbert, and B. C. Bullock. 1987. Alteration of high density lipoprotein subfractions of nonhuman primates fed fish-oil diets. Selective lowering of HDL subfractions of intermediate size and density. *Arteriosclerosis.* **7:** 71–79.
13. Parks, J. S., B. C. Bullock, and L. L. Rudel. 1989. The reactivity of plasma phospholipids with lecithin:cholesterol acyltransferase is decreased in fish oil-fed monkeys. *J. Biol. Chem.* **264:** 2545–2551.
14. Parks, J. S., T. Y. Thuren, and J. D. Schmitt. 1992. Inhibition of lecithin:cholesterol acyltransferase activity by synthetic phosphatidylcholine species containing eicosapentaenoic acid or docosahexaenoic acid in the *sn*-2 position. *J. Lipid Res.* **33:** 879–887.
15. Parks, J. S., and T. Y. Thuren. 1993. Decreased binding of apoA-I to phosphatidylcholine (PC) monolayers containing 22:6 n–3 in the *sn*-2 position. *J. Lipid Res.* **34:** 779–788.
16. Rainwater, D. L., D. W. Andres, A. L. Ford, W. F. Lowe, P. J. Blanche, and R. M. Krauss. 1992. Production of polyacrylamide gradient gels for the electrophoretic resolution of lipoproteins. *J. Lipid Res.* **33:** 1876–1881.
17. Verdery, R. B., D. F. Benham, H. L. Baldwin, A. P. Goldberg, and A. V. Nichols. 1989. Measurement of normative HDL subfraction cholesterol levels by Gaussian summation analysis of gradient gels. *J. Lipid Res.* **30:** 1085–1095.
18. Miller, K. R., J. Wang, M. Sorci-Thomas, R. A. Anderson, and J. S. Parks. 1996. Glycosylation structure and enzyme activity of lecithin:cholesterol acyltransferase from human plasma, Hep G2 cells, and baculoviral and Chinese hamster ovary cell expression systems. *J. Lipid Res.* **37:** 551–561.
19. Lowry, O. H., N. J. Rosebrough, A. L. Farr, and R. J. Randall. 1951. Protein measurement with the Folin phenol reagent. *J. Biol. Chem.* **193:** 265–275.
20. Yang, C. Y., D. Manoogian, Q. Pao, F. S. Lee, R. D. Knapp, A. M. Gotto, Jr., and H. J. Pownall. 1987. Lecithin:cholesterol acyltransferase. Functional regions and a structural model of the enzyme. *J. Biol. Chem.* **262:** 3086–3091.
21. Chen, Y., J. T. Yang, and H. M. Martinez. 1972. Determination of the secondary structures of proteins by circular dichroism and optical rotatory dispersion. *Biochemistry.* **11:** 4120–4131.
22. Sparks, D. L., S. Lund-Katz, and M. C. Phillips. 1992. The charge and structural stability of apolipoprotein A-I in discoidal and spherical recombinant high density lipoprotein particles. *J. Biol. Chem.* **267:** 25839–25847.
23. Pace, C. N. 1986. Determination and analysis of urea and guanidine hydrochloride denaturation curves. *Methods Enzymol.* **131:** 266–280.
24. Thornburg, J. T., J. S. Parks, and L. L. Rudel. 1995. Dietary fatty acid modification of HDL phospholipid molecular species alters lecithin:cholesterol acyltransferase reactivity in cynomolgus monkeys. *J. Lipid Res.* **36:** 277–289.
25. Bolin, D. J., and A. Jonas. 1994. Binding of lecithin:cholesterol acyltransferase to reconstituted high density lipoproteins is affected by their lipid but not apolipoprotein composition. *J. Biol. Chem.* **269:** 7429–7434.
26. Wald, J. H., E. S. Krul, and A. Jonas. 1990. Structure of apolipoprotein A-I in three homogeneous, reconstituted high density lipoprotein particles. *J. Biol. Chem.* **265:** 20037–20043.
27. Sparks, D. L., W. S. Davidson, S. Lund-Katz, and M. C. Phillips. 1993. Effect cholesterol on the charge and structure of apolipoprotein A-I in recombinant high density lipoprotein particles. *J. Biol. Chem.* **268:** 23250–23257.
28. Sparks, D. L., W. S. Davidson, S. Lund-Katz, and M. C. Phillips. 1995. Effects of the neutral lipid content of high density lipoprotein on apolipoprotein A-I structure and particle stability. *J. Biol. Chem.* **270:** 26910–26917.
29. Jonas, A., J. H. Wald, K. L. Toohill, E. S. Krul, and K. E. Kezdy. 1990. Apolipoprotein A-I structure and lipid properties in homogeneous, reconstituted spherical and discoidal high density lipoproteins. *J. Biol. Chem.* **265:** 22123–22129.
30. Holte, L. L., S. A. Peter, T. M. Sinnwell, and K. Gawrisch. 1995. ^{2}H nuclear magnetic resonance order parameter profiles suggest a change of molecular shape for phosphatidylcholines containing a polyunsaturated acyl chain. *Biophys. J.* **68:** 2396–2403.
31. Ho, C., S. J. Slater, and C. D. Stubbs. 1995. Hydration and order in lipid bilayers. *Biochemistry.* **34:** 6188–6195.
32. Litman, B. J., and D. C. Mitchell. 1996. A role for phospholipid polyunsaturation in modulating membrane protein function. *Lipids.* **31:** S193–S197.
33. Slater, S. J., M. B. Kelly, M. D. Yeager, J. Larkin, C. Ho, and C. D. Stubbs. 1996. Polyunsaturation in cell membranes and lipid bilayers and its effects on membrane proteins. *Lipids.* **31:** S189–S192.
34. Holte, L. L., F. Separovic, and K. Gawrisch. 1996. Nuclear magnetic resonance investigation of hydrocarbon chain packing in bilayers of polyunsaturated phospholipids. *Lipids.* **31:** S199–S203.
35. Wolfe, M. S., J. S. Parks, T. M. Morgan, and L. L. Rudel. 1993. Childhood consumption of dietary polyunsaturated fat lowers risk for coronary artery atherosclerosis in African green monkeys. *Arterioscler. Thromb.* **13:** 863–875.
36. Rudel, L. L., J. S. Parks, F. L. Johnson, and J. Babiak. 1986. Low density lipoproteins in atherosclerosis. *J. Lipid Res.* **27:** 465–474.
37. Mattson, F. H., and S. M. Grundy. 1985. Comparison of effects of dietary saturated, monounsaturated, and poly-

unsaturated fatty acids on plasma lipids and lipoproteins in man. *J. Lipid Res.* **26:** 194–202.
38. Grundy, S. M., D. Nix, M. F. Whelan, and L. Franklin. 1986. Comparison of three cholesterol-lowering diets in normolipidemic men. *J. Am. Med. Assoc.* **256:** 2351–2355.
39. Babiak, J., F. T. Lindgren, and L. L. Rudel. 1988. Effects of saturated and polyunsaturated dietary fat on the concentrations of HDL subpopulations in African green monkeys. *Arteriosclerosis.* **8:** 22–32.
40. Schonfeld, G., W. Patsch, L. L. Rudel, C. Nelson, M. Epstein, and R. E. Olson. 1982. Effects of dietary cholesterol and fatty acids on plasma lipoproteins. *J. Clin. Invest.* **69:** 1072–1080.
41. Horowitz, B. S., I. J. Goldberg, J. Merab, T. M. Vanni, R. Ramakrishnan, and H. N. Ginsberg. 1993. Increased plasma and renal clearance of an exchangeable pool of apolipoprotein A-I in subjects with low levels of high density lipoprotein cholesterol. *J. Clin. Invest.* **91:** 1743–1752.
42. Shepherd, J., A. M. Gotto, Jr., O. D. Taunton, M. J. Caslake, and E. Farish. 1977. The in vitro interaction of human apolipoprotein A-I and high density lipoproteins. *Biochim. Biophys. Acta.* **489:** 486–501.
43. Parks, J. S., and L. L. Rudel. 1982. Different kinetic fates of apolipoproteins A-I and A-II from lymph chylomicra of nonhuman primates. Effect of saturated versus polyunsaturated dietary fat. *J. Lipid Res.* **23:** 410–421.